On the Existence of Low-Dimensional Chaos of Tropical Cyclone Intensity

Chanh Kieu[1] *

[1]*Department of Earth and Atmospheric Sciences, Indiana University, Bloomington, IN 47405.*

Weiran Cai[1,2]

[2]*Department of Mathematics, Indiana University, Bloomington, IN 47405.*

Wai-Tong Louis Fan[2,3]

[3]*Center of Mathematical Sciences and Applications, Harvard University, Cambridge, MA 02138.*

**Corresponding author address:* Chanh Kieu. Department of Earth and Atmospheric Sciences, Indiana University, Bloomington, IN 47405.

E-mail: ckieu@indiana.edu

ABSTRACT

This study examines the potential limit in the reliability of tropical cyclone (TC) intensity prediction. Using the phase-space reconstruction method for TC intensity time series, it is found that TC dynamics contains low-dimensional chaos at the maximum intensity equilibrium. Examination of several attractor invariants including the largest Lyapunov exponent, the Sugihara-May correlation, and the correlation dimension captures a consistent range of the chaotic attractor dimension between 4-5 for TC intensity. In addition, the error doubling time estimated from the largest Lyapunov exponent for TC intensity is roughly 1-3 hours, which accords with the decay time obtained from the Sugihara-May correlation at the maximum intensity equilibrium. Furthermore, the findings in this study reveal a relatively short limit for TC intensity predictability based on the traditional maximum surface wind, which is $\sim$3-9 hours after reaching the mature stage, but noticeably longer for the minimum central pressure ($\sim$12-18 hours). So long as the traditional metrics for TC intensity such as the maximum surface wind or the minimum central pressure is used for intensity forecast, our results support that TC intensity forecast errors will not be reduced indefinitely in any operational model, even in the absence of all model and observational errors. As such, the future improvement of TC intensity forecast should be based on different metrics beyond the absolute intensity errors that are currently used in real-time intensity verification.

1. Introduction

Quantifying how far in advance one can predict weather or climate, the so-called atmospheric predictability, is a vital question in real-time forecast. With a wide range of atmospheric systems and operational requirements, there exits however no single method to determine the predictability for all weather phenomena and variables. For example, a large-scale weather system has a typical limit of 2 weeks for geopotential height (Lorenz 1969, 1990, 1996; Leith 1971; Métais and Lesieur 1986), yet the predictability for rainfall rate or mesoscale cluster development could be much shorter (Zhang et al. 2003; Durran et al. 2013). Likewise, weather extremes such as tornadoes or convective-scale thunderstorms often cannot be predicted a few hours ahead (Hart and Cohen 2016a; Stensrud et al. 01 Oct. 2009; Bunker et al. 01 Apr. 2019). Therefore, a question of what is the maximum time range that one can reliably predict tropical cylone (TC) intensity or track is non-trivial.

Among many difficulties in understanding TC predictability, one central issue roots in the definition of predictability itself. Formally, the predictability of a variable is defined as a maximum time interval beyond which the forecast distribution of that variable becomes indistinguishable from its climatological distribution (Lorenz 1969; Shukla 1981; Schneider and Griffies 1999; DelSole 01 Oct. 2004; DelSole and Tippett 2007). From this formal definition, it is apparent that predictability must be associated with one specific variable over a given period during which the climatology of the variable is constructed. Thus, predictability is not a universal metric but varies for different variables and different constructions of climatology (DelSole and Tippett 2007).

Given such metric-dependence of predictability, any analysis of TC predictability must be therefore carried out for one particular aspect such as track, intensity, decadal shift in the maximum intensity, or seasonal TC frequency. Recent studies by Kieu and Moon (2016); Kieu et al. (2018,

2021) proposed that TC dynamics should possess low-dimensional chaos in order to account for the intensity error saturation at 4-5 day lead times as observed in real-time intensity verification. Using TC-scale phase space and estimation from idealized simulations, they suggested the size of the TC intensity chaotic attractor varies in the range of 3-10 ms^{-1}, depending on TC models. Due to various simplifications and uncertainties in their TC-scale framework as well as real-time TC analyses, the limit of intensity predictability related to such intrinsic TC chaotic dynamics is still inconclusive and the estimation of such an intensity predictability limit still remains open.

Because TCs are a complex dynamics system, examining their full dynamics from a strict mathematical perspective is unfeasible at present. This is especially apparent in current numerical models, which contain various nonlinear interactions among different physical parameterizations. In this study, we wish to use the phase-space reconstruction method in nonlinear dynamics to examine an important question of TC intensity predictability limit. By analyzing the output of TC intensity from a long simulation, our ultimate goal is to establish more affirmatively that TC dynamics is inherently chaotic at the maximum intensity equilibrium. The ability to state that TC intensity has intrinsic chaos is very significant, because it is critical for future real-time TC forecast, model development planning, or risk management. Thus, quantifying the properties of TC intensity intrinsic chaos will allow one to obtain a proper range of TC intensity predictability for operational forecasts.

The rest of this work is organized as follows. In the next, the methods for detecting chaos by using the phase-space reconstruction techniques as well as detailed experiment descriptions are provided. Section 3 presents our analyses of TC intensity time series from several different angles of chaotic dynamics, while Section 4 discusses some issues related to the phase-space reconstruction method. Concluding remarks are then given in the final section.

2. Methods

a. Phase-space reconstruction

In a strict mathematical sense, the governing equations for TCs are not closed due to our incomplete understanding of TC dynamics and thermodynamics. As a consequence, all current representations of TC processes in numerical models must employ empirical parameterizations that only approximate the true TC physics. These physical parameterizations generally contain many uncertainties and simplifications, which prevent one from fully understanding TC development.

Early works by Takens and many others (Takens 1981; Brock 1986; Theiler 1987; Sugihara and May 1990; Sugihara et al. 1994; Casdagli 1992) have shown, however, that the dynamics of a nonlinear system can be reconstructed from a single time series of a state variable under some specific conditions, even in the absence of complete governing equations for the system. Assuming that a nonlinear system possesses low-dimensional chaos at its statistically stationary state, it is in fact possible to examine multidimensional phase portraits of a chaotic attractor by reconstructing the attractor in the phase space of time-lagged coordinates. With this phase-space reconstruction, different invariants of the original chaotic attractor can be effectively obtained once the embedding dimension and time delay are properly chosen Kantz and Schreiber (2003).

There are a range of techniques that have been proposed to find a proper embedding dimension and time delay for phase-space reconstruction such as the averaged mutual information, autoregression, or false nearest neighborhood (Fraser and Swinney 1986; Sugihara et al. 1994; Kantz and Schreiber 2003; Wallot and Monster 2018). These methods all share a common principle that basic invariants of a chaotic attractor must be intrinsic, regardless of the reconstruction methods if the embedding dimension and time lag are correct. Among several approaches to detect chaos in a phase space reconstructed from a time series, we will present in this study several measures that

most characterize the deterministic chaos, which include the largest Lyapunov exponent (LLE), the Sugihara and May (1990)'s correlation (SMC) curve, and the correlation dimension.

For the LLE measure, an early algorithm for computing LLE from a given time series was first proposed by Wolf et al. (1985), which has been later improved in many subsequent studies (Rosenstein et al. 1993; Kantz 1994; Balcerzak et al. 2018; Awrejcewicz et al. 2018). For our implementation of the LLE algorithm, a modified version of Wolf's algorithm presented in Brock (1986) was chosen because of its efficiency. The basic steps of Brock's scheme are summarized below (see the full proof of the LLE convergence in Brock (1986)):

- Step 1: From a given time series $\{a_i\}, i = 1...N$ where N is the number of data sampling, generate a set of m-history $a_t^m \equiv \{a_t, a_{t+\tau}, ..., a_{t+(m-1)\tau}\}, t = 1...N_m \equiv N-(m-1)\tau$ for the phase-space reconstruction, with a given time delay τ and an embedding dimension m;

- Step 2: Initialize an error growth cycle by finding the nearest neighborhood $a_{t_1}^m$ of the first m-history a_1^m such that $a_{t_1}^m \neq a_1^m$;

- Step 3: Choose a prescribed evolution window q and compute $g_1(q) = d_2(1)/d_1(1)$, where $d_1^{(1)} = \|a_{t_1}^m - a_1^m\|$ and $d_2^{(1)} = \|a_{t_1+q}^m - a_{1+q}^m\|$ are distances in the reconstructed phase space with a given metric $\|\cdot\|$;

- Step 4: Perform a loop from $k = 2$ to $K = max\{k \,|\, 1+kq \leq N_m\}$ that repeatedly does the following two main tasks:

  1. Find an index t_k of t to minimize a penalty function $p(a_t^m - a_{1+(k-1)q}^m, a_{t_{k-1}+q}^m - a_{1+(k-1)q}^m)$ defined as follows:

$$p(a_t^m - a_{1+(k-1)q}^m, a_{t_{k-1}+q}^m - a_{1+(k-1)q}^m) = \|a_t^m - a_{1+(k-1)q}^m\| + w|\theta(a_t^m - a_{1+(k-1)q}^m, a_{t_{k-1}+q}^m - a_{1+(k-1)q}^m)|,$$

where w is a weighted parameter for the deviation angle θ.

2. Compute and store the divergence rate of the kth loop defined as $g_k(q) = d_2(k)/d_1(k)$, where $d_1(k) = \|a^m_{t_k} - a^m_{1+(k-1)q}\|$, $d_2(k) = \|a^m_{t_k+q} - a^m_{1+kq}\|$.

- Step 5: Finally, compute LLE λ_q by averaging all $g_k(q)$ as $\lambda_q = \frac{1}{K}\Sigma_{k=1}^{K}\frac{\ln(g_k(q))}{q}$.

We should mention that all LLE algorithms assume *a priori* the values of the embedding dimension m and the time delay τ. These values are generally not known in advance, given a time series of a state output. While one can always search for (m,τ) using existing algorithms such as the false nearest neighbor or mutual information method (Fraser and Swinney 1986; Sugihara et al. 1994; Rhodes and Morari 1997; Wallot and Monster 2018) , it should be noted that the above LLE's algorithm must converge to a correct LLE of a chaotic attractor with a fractal dimension n, if it exists, for $m > 2n+1$ as proven in Brock (1986). As such, one can plot $\lambda(q)$ as a function of (m,τ) and search for the values of (m,τ) for which LLE becomes stabilized. This approach of searching for a LLE in the parameter space (m,τ) is chosen in this study, because it can help reduce various prescribed thresholds for (m,τ) in the current LLE algorithms as also discussed in Kantz and Schreiber (2003).

Along with LLE, Sugihara and May (1990) proposed another measure to detect chaos that is also of particular interest because of its simplicity and effectiveness. The main idea behind Sugihara and May (1990)'s approach is that a chaotic time series should possess limited predictability, whereas true stochastic variation would have no predictability. Practically, this important property of chaotic time series implies that the correlation between model forecast and observations must decay with time in a chaotic system.

For the sake of completeness, we summarize here the main step to obtain the Sugihara-May correlation as a function of forecast lead time (T) from a given time series. Detailed discussion

of this method as well as its variation can be found in Sugihara and May (1990); Sugihara et al. (1994); Kantz and Schreiber (2003) and so will not be duplicated here.

- Step 1: Given a time series $\{a_i\}, i = 1...N$, one first divides it into an "atlas" (or training) set $\mathscr{A}$ and a test set $\mathscr{T}$;

- Step 2: Reconstruct a phase space with a given embedding dimension m by generating the m-histories obtained from lagged time series as $a_t^m = (a_t, a_{t+\tau}, \ldots, a_{t+(m-1)\tau})$ for both sets $\mathscr{A}, \mathscr{T}$;

- Step 3: For each history $a_i^m \in \mathscr{T}$ (the so-called predictee in Sugihara and May) in the m-dimensional space, search for n_b neighbouring points in $\mathscr{A}$ with the minimal distance to a_i^m such that the predictee are within a smallest simplex spanned by these n_b neighbouring points;

- Step 4: choose a lead time T, and a prediction for a_i^m at the lead time T can be then obtained by projecting the entire simplex into the future at leading time T, denoted $a_{i(j)}^f(T)$, where $j = 1...n_b$. The prediction value at lead time T for a_i^m, denoted by $\bar{a}_i^f(T)$, is then computed by taking an ensemble average of n_b values of $a_{i(j)}^f(T)$;

- Step 5: construct a pair between the prediction $a_i^f(T)$ and the actual value of a_i^m evolution after T steps forward that is obtained directly from the training set $\mathscr{T}$, i.e., $a_{i+T}^m \in \mathscr{T}$;

- Step 6: Repeat Steps 3-5 for all data points $a_i \in \mathscr{T}$ and obtain the correlation $\rho(T)$ between $(\bar{a}_i^f(T), a_{i+T}^m)$ for each lead time T;

- Step 7: Repeat Steps 3-6 for different values of T to obtain the curve $\rho(T)$ as a function of T.

Note that in Step 4 of the above SMC algorithm, there are several different ways to obtain $\bar{a}_i^f(T)$ (also known as "the prediction model") such as weighted average, regression combination, ensemble average, or neural network. Regardless of the prediction model, the key property of any

chaotic time series is that $\rho(T)$ must decay with lead time T in the presence of low-dimensional chaos. In this regard, the SMC curve $\rho(T)$ comprises a criterion for detecting chaotic time series; a deterioration of SMC with the leading time indicates the existence of chaos, whereas a purely stochastic time series would have a constant SMC regardless of how far into the future. More verification and applications of SMC for different systems can be found in Sugihara and May (1990); Sugihara et al. (1994).

Similar to the LLE algorithm, both the embedding dimension m and the delay time τ have to be given before computing SMC. Our proposed approach to this freedom in choosing these parameters is to again generate an SMC curve $\rho(T)$ for a range of values of (m, τ) as for the LLE analyses. The convergence of the SMC curve for some domain in the (m, τ) parameter space will then indicate the existence of a low-dimensional chaotic attractor in the embedding phase space. By comparing the values of (m, τ) obtained from the convergence of the SMC curves to the values of (m, τ) obtained from the convergence of LLE, one can then further estimate a proper range for (m, τ) that represents the chaotic regime of TC intensity. More in-depth discussion about other methods for choosing optimal parameters (m, τ) can be found in Grassberger et al. (1991).

b. Idealized TC simulations

Given our approaches of searching for chaos from time series described in the previous section, the next step is to generate a time series of TC intensity for the phase-space reconstruction analysis. In principle, one could obtain this time series directly from observation such as flight data or satellite imagery. However, the requirement of a stationary time series for the phase-space reconstruction imposes a strong constraint on possible choices of time series, as real TC intensity contain various stages of TC development in different environments instead of just the mature stage. As such, using a TC model to produce the intensity time series in a fixed environment is the

most apparent approach for our purpose. Ideally, one should use full-physics three-dimensional models that are as much realistic as possible such as the Hurricane Weather Research and Forecasting (HWRF) model. These types of limited-area models are, nevertheless, designed on a rectangle domain with strong constraints by lateral boundary conditions that prevent one from running for a very long time to generate a stationary time series. Because of this, we choose herein an idealized model that allows for a long integration without the issue of lateral boundary asymmetries.

In this regard, the axisymmetric configuration of the cloud model (CM1, Bryan and Fritsch (2002)) was used to generate different intensity time series for our phase-space analyses. The model was configured with 359 grid points on a stretching grid in the radial direction with the highest resolution of 2 km in the storm central region and stretched to 6 km outside 1000 km radius. In the vertical direction, a setting of 61 levels with a fixed resolution of 0.5 km was chosen. The model was initialized from the tropical Jordan sounding on an f-plane, with fixed sea surface temperature (SST) = 302.15 K.

Because of the requirement of a quasi-stationary time series at the maximum intensity equilibrium, the model was configured for 100-day simulations. A stable maxiimum intensity equilibrium for this 100-day integration could be obtained by using a suite of physical paramterizations including the YSU boundary layer scheme, the TKE subgrid turbulence scheme, and explicit moisture Kessler scheme with no cumulus parameterization. For the radiative parameterization, an idealized option with the Newtonian cooling relaxation of 2 K day^{-1} was applied, similar to what used in Kieu and Moon (2016). This choice of the radiative cooling parameterization is sufficient to allow for a stable maximum intensity equilibrium during the entire 100-day simulations as shown in Figure 1. Given this stable configuration of TC intensity, the time series of U_{MAX}, V_{MAX}, W_{MAX}, and P_{MIN} were then output at an ultra-high sampling frequency of 36 seconds to maximize our time series analyses.

As a step to further verify the effects of random noise on our analyses, a set of sensitivity experiments were also conducted for which random white noise with a given variance was added to the CM1 model forcing at every time step. This implementation of additive random noise turns the CM1 model into a stochastic system whose output now contains random fluctuations with an amplitude proportional to the magnitude of random forcing. As discussed in Nguyen et al. (2020), this additive random noise in terms of the Wiener process results in a first-order accuracy for the CM1 finite difference scheme, similar to the Euler-Maruyama method. By choosing a sufficiently small time step, the model is able to maintain its numerical stability for a range of experiments. Note that random noise was applied only to wind components at all CM1 grid points, with an variance in the range of $[10^{-3} - 10^{-1} ms^{-1}]$. Beyond this range, we notice that the model violates the CFL conditions and quickly loses its stability after just a few steps of integration. The main rationale for applying random noise only to the wind field in these sensitivity experiments is because wind components generally most fluctuate with time at any grid point. Adding random noises to the model temperature, pressure, and moisture fields does not change the outcomes, yet these extra noises would cause the model to become more unstable and limit the range of random noise amplitude that we can implement for the wind components. Thus, all stochastic simulations were carried out only for the wind perturbations in this study.

3. Results

Given the traditional practice of forecasting TC intensity based on the maximum 10-m wind (V_{MAX}) and the minimum central pressure (P_{MIN}), the time series of these two metrics is required to reconstruct a TC intensity phase space for our analyses. While a single time series of V_{MAX} or P_{MIN} may appear to be too little to explore the complex dynamics of hurricanes, the powerful phase-space reconstruction theorem by Takens (1981) ensures that any single time series should

contain rich information about the underlying dynamics if low-dimensional chaos exists. That is, one can explore the main properties of a chaotic attractor for TC intensity from any time series, regardless of the output variables (Wolf et al. 1985; Fraser and Swinney 1986; Brock 1986; Theiler 1987; Sugihara and May 1990; Casdagli 1992; Sugihara et al. 1994; Wallot and Monster 2018). Because of this, our aim here is to explore to what degree the TC dynamics contain intrinsic low-dimensional chaos at the maximum intensity limit that can account for intensity limited predictability as proposed in recent studies.

a. Existence of maximum intensity equilibrium

Since the phase-space reconstruction method requires a stationary time series, it is necessary to examine first if the maximum intensity equilibrium exists during TC development. In this regard, Figure 1a shows the time series of the maximum surface wind speed obtained from an 100-day simulation, using the CM1 model. One notices in Figure 1a that the model vortex experiences a brief rapid intensification during the first 3-5 days and quickly settles down to a mature state after 9-10 days into the model integration. These behaviors are typical in TC development under idealized conditions as shown in various studies (see, e.g., Rotunno and Emanuel 1987; Wang 2001; Bryan and Rotunno 2009; Hakim 2011, 2013; Davis 2015; Kieu and Moon 2016). Although the quasi-stationary equilibrium at the maximum intensity is evident in our simulation as seen in Figure 1, we note that the existence of such a stable equilibrium is still an open question from the practical standpoint due to the sensitivity of this equilibrium to model configurations and environmental assumptions (Montgomery et al. 2009; Hakim 2011; Kieu and Moon 2016). However, with the experiment settings described in Section 2, the stable equilibrium of the model maximum

intensity (MMI[1]) can be well captured and maintained during the entire 100-day period, which suffices for us to examine the phase-space reconstruction for TC intensity as expected.

Given the MMI equilibrium, it is apparent that the maximum intensity does not take one single value but highly fluctuates with time, similar to what obtained in previous studies (Hakim 2011, 2013; Kieu and Moon 2016). As shown in Figure 1, temporal fluctuations at the MMI equilibrium are observed not only for V_{MAX} but also for other variables including P_{MIN}, the maximum boundary-layer inflow (U_{MAX}), and the maximum vertical motion in the eyewall region (W_{MAX}). From the statistical standpoint, these fluctuations show no obvious difference between chaotic and stochastic variability, thus highlighting an important question in TC dynamics: do these fluctuations reflect the low-dimensional deterministic chaos of TC intensity, model random truncation errors, or a manifestation of high-dimensional nonlinearity projection (the so-called process or stochastic noise in Sugihara et al. (1994); Casdagli (1992))?

From the time series output, it should be noted that all numerical models appear to be stochastic (Kantz and Schreiber 2003; Nguyen et al. 2020). This is because numerical truncation errors can be amplified by nonlinearity and projected onto the time series, resulting in an unexplained noise in the model output (Brock 1986; Casdagli 1992; Sugihara et al. 1994; Kantz and Schreiber 2003). This stochastic nature of model time series is especially true for modern modelling systems, which employ also various stochastic paramterization schemes or random switches such as convective triggering mechanism (Palmer 2001; Christensen et al. 2015; Dorrestijn et al. 2015; Zhang et al. 2015). As such, the strong fluctuation of TC intensity as shown in Figure 1 is always present for any model output.

There are several different techniques in nonlinear time series analyses that can address the distinction between deterministic or stochastic variability as extensively detailed in Kantz and

[1]It should be noted that MMI is generally different from the theoretical potential intensity limit obtained in Emanuel (1986).

Schreiber (2003). In this study, with a large sample size of the TC intensity state at the MMI equilibrium, we can directly examine the nonlinear chaotic invariants by dividing the long dataset into many smaller overlapped patches, the so-called a sliding window detector method in data analysis, to increase the reliability of our estimation. Specifically in this study, three key measures of deterministic chaos to be examined are i) the largest Lyapunov exponent, ii) the Sugihara-May correlation, and iii) the correlation dimension for TC intensity. These are the main invariants of any chaotic attractor, which can help answer the main question of the potential existence of low-dimensional chaos for TC intensity that we wish to explore in this study.

b. Largest Lyapunov exponent

To examine the nature of the variability in the V_{MAX}, U_{MAX}, W_{MAX}, and P_{MIN} time series, Figure 2 shows the largest Lyapunov exponent (LLE) λ as a function of embedding dimension m, which is obtained for a range of delay time (τ) between 10-60 minutes. Note that this range of τ is based on the nature of TC dynamics process, which is strongly governed by convective activities at a time scale of minutes to hours. As discussed in Kantz and Schreiber (2003), the choice of τ should have minimum effects on the attractor invariants if the phase-space reconstruction is effective. Thus, it is important to see how sensitive the LLE estimations are to different delay times. Of course, a positive LLE is necessary but not sufficient to conclude whether the variability in a time series is a result of low-dimensional chaos or not. However, the existence of such a positive LLE is a required condition that any chaotic system must possess and so we need to examine it first (Wolf et al. 1985; Fraser and Swinney 1986; Theiler 1987; Brock 1986; Sugihara et al. 1994).

One notices two important features from Figure 2. First, the LLEs derived from all time series display a consistent behavior for all τ between 10-60 minutes, with a decrease of LLE for larger embedding dimension (m) and subsequent leveling off in the range of $0.5 - 1.4 \times 10^{-4} s^{-1}$ for

$m \geq 10$. Note that an LLE of $1 \times 10^{-4} s^{-1}$ is equivalent to a doubling time of ~ 3 hours in the full physical dimension. Thus, the range of LLEs shown in Figure 2 suggests that an initial error would be doubled every 1-5 hours at the maximum intensity equilibrium. While this is relatively broad range, it is important that all LLEs are positive and convergent towards a stable range when m increases. Specifically, the decaying of LLEs with m as seen in Figure 2 suggests that small embedding dimension $m < 10$ would not properly capture TC intensity chaotic attractor. As m increases, attractor invariants such as LLEs must converge towards a more stable value, if a low-dimensional chaotic attractor truly exists. In this regard, the decay of LLEs with m in Figure 2 provides some initial indication about possible existence of intensity chaos that we wish to quantify next.

Second, Figure 2 shows further that all LLEs converge towards a stable value for the embedding dimension $m \geq 10$, regardless of the variables or time delay values used to reconstruct the phase space. Although the value of the stable LLE cannot be precisely pinpointed due to wide range between $0.5 - 1.4 \times 10^{-4} s^{-1}$, the fact that such a stable value for LLE exists for $m \geq 10$ is important here. Namely, this convergence of LLEs implies that a low-dimensional chaotic attractor of TC intensity has an intrinsic dimension $n \approx 4 - 5$, according to the Takens embedding theorem [2]. Of course, finding the exact embedding dimension m from a given time series that can ensure the Takens theorem is difficult, because this embedding dimension is often ad-hoc and dependent on choices of parameters such as time delay, sampling frequency, or sample size (Kantz and Schreiber 2003). Nevertheless, our sensitivity estimation of m using different methods such as the false nearest neighbor (FNN) method (Fraser and Swinney 1986; Sugihara et al. 1994; Wallot

[2]Note that phase space reconstruction generally requires a minimum dimension $m = 2n + 1$, where n is the dimension of the attractor, such that the invariants of the attractor can be properly estimated. This attractor dimension n is independent of the embedding space dimension m for $m \geq 2n + 1$. See a proof in Brock (1986).

and Monster 2018) captures a similar minimum range for $m \in [10-14]$. Thus, it is expected that the intensity chaotic attractor would require a minimum embedding dimension $m \sim 10$ for the TC intensity phase-space reconstruction as shown in Figure 2.

It is of interest to note however a distinct behavior of the LLE estimation from Figure 2 that the LLE appears to be quite different between the wind (i.e., U_{MAX}, V_{MAX}, and W_{MAX}) and the pressure (i.e., P_{MIN}) time series. Specifically for the CM1 simulations herein, LLE is $\sim 0.5-1.4\times10^{-4}s^{-1}$ for V_{MAX}, U_{MAX}, or W_{MAX}, but it is noticeably smaller ($\sim 0.1-0.5\times10^{-4}s^{-1}$) for P_{MIN}. In addition, the convergence of LLE for the P_{MIN} time series occurs for $m \geq 16$ as compared to $m \geq 10$ for the wind time series. Such difference between LLEs obtained from the wind and the pressure variables may reflect different predictability for different state variables in a multi-scale system with the co-existence of fast and slow-varying processes (Shukla 1981; Goswami et al. 01 May. 1997; Lorenz 15 Dec. 1992; DelSole et al. 15 May. 2017). Much like the predictability of rainfall is different from that of temperature or 500-hPa geopotential for the same large-scale weather systems, it is possible that the TC pressure and wind fields possess inherently different predictability ranges. This can help explain why recent studies have proposed to use P_{MIN} as a measure for TC intensity in operational forecast instead of V_{MAX}, because it potentially allows for more reliable intensity forecast in the long run (see, e.g., Klotzbach et al. 2020).

While our search for the minimum embedding dimension based on the convergence of LLEs differs from other approaches such as the box counting or the correlation dimension method (Nicolis and Nicolis 1984; Brock 1986; Casdagli 1992), we note that all phase-space reconstruction methods are somewhat subjective and similarly ad-hoc due to the wide range of nonlinear dynamical systems and time series characteristics (Kantz and Schreiber 2003). Thus, there is always some uncertainty in determining a proper minimum dimension for embedding phase space, which explains why m has a range of 10-16 or LLEs $\sim 0.5-1\times10^{-4}\ s^{-1}$ as seen in Figure 2. Regardless of

this uncertainty, the emergence of low-dimensional chaos for TC intensity with a relatively small value of m is still noteworthy, since a large embedding dimension would imply that our time series analysis is insufficient to capture chaotic dynamics [3]. From this perspective, the LLE analyses herein could provide some evidence of low-dimensional chaos for TC intensity, at least from the standpoint of error growth on an attractor at the quasi-stationary equilibrium.

c. Sugihara-May correlation

As discussed in Sugihara et al. (1994), detecting chaos based on the existence of a positive LLE in any time series must be cautioned. This is because any fluctuation in a time series could be manifestation of high-dimension nonlinearity or random noise. One could indeed have a non-chaotic system with a positive LLE if there is sufficiently large random noise in the time series (Brock 1986; Casdagli 1992; Sugihara et al. 1994). As such, a positive LLE as shown in Figure 2 may not be insufficient to guarantee the existence of low-dimensional chaos.

To further examine the potential low-dimensional chaos in TC intensity time series, Figure 3 shows the Sugihara-May correlation (SMC) as a function of forecast lead time T for all four variables. Again, SMC is obtained by using a modified version of Sugihara and May's original algorithm, in which the forecast scheme is based on an ensemble average instead of a weighted sum (Sugihara and May 1990) or regression method (Casdagli 1992) as described in the Method section. Note also that a fixed embedding dimension $m = 10$ and the delay time $\tau = 30$ minutes are chosen for this SCM calculation, based on the results from the LLE analyses in the previous section.

[3] As discussed in Casdagli (1992), a high-dimensional deterministic chaos would be in fact manifested as stochastic variability, even in the absence of all random noise.

One notices in Figure 3 that SMCs from all four different variables show rapid decay with forecast lead time. As discussed in Sugihara and May (1990), this type of decaying correlation is a characteristic of chaotic dynamics, which is distinct from the pure random noise variability whose SMC is statistically constant. Of further interest in Figure 3 is the consistency of such decaying SMC among all time series, which confirms the limited predictability for TC intensity due to the low-dimensional chaos, irrespective of model output. Specifically for our CM1 simulation, we observe that SMC decreases from 1.0 to about 0.1 after reaching a limit $T^* \approx$ 3-5 hours for the wind variables and 12-18 hours for the pressure variable. Such a chaotic decorrelation time is also consistent with the predictability range obtained from the TC energy spectral analyses in Kieu and Rotunno (2022) at the maximum intensity equilibrium.

Similar to the LLE analyses, the time series for the wind components (U_{MAX}, V_{MAX}, W_{MAX}) display a consistent range of predictability among themselves ($T^* \approx$ 3-5 hours), while P_{MIN} tends to capture a longer decorrelation time ($T'^* \approx$ 12-18 hours) as shown in Figure 3. This difference in SMC between the pressure and the wind time series is robust for a range of embedding dimension, delay time, model physical options, stochastic forcings, or initial conditions in our analyses, so long as the phase space is properly reconstructed. Such a longer decorrelation time in the P_{MIN} time series again suggests that the pressure field may contain different dynamics, which may allow for more reliable intensity forecast at longer lead times. The fact that both LLE and SMC analyses provide such a consistently different behavior between the wind and pressure variables highlights the possible different predictability for TC intensity when using V_{MAX} or P_{MIN} as suggested in the previous studies.

Our additional analyses with different delay time τ or embedding dimension m confirm that the SMC curves display consistent decay and level off only when $m \geq 10$, which is comparable with the embedding dimension obtained from the LLE convergence for the wind field or FNN method

(not shown). For smaller values of m, the SMC curve does not posses a monotonic decay but highly fluctuates with forecast lead time. These analyses reiterate the results from the LLE analyses that the embedding dimension for TC intensity phase space must be sufficiently large before one can attain consistent characteristics of SMC.

d. Correlation dimension

The consistent convergences of the SMC curve and the LLE for $m \geq 10$ is noteworthy, because it suggests the existence of a low-dimensional attractor with dimension $n \sim 4-5$ from the Takens theorem. To directly verify this intrinsic dimension of the TC intensity chaotic attractor, the Grassberger-Procaccia (GP) correlation dimension algorithm Theiler (1987) is used to estimate the dimension of the TC intensity attractor directly from the CM1 time series (Figure 4a) [4]. While this correlation dimension algorithm has some degree of subjectivity in choosing the best linear fit for correlation integral, these correlation integral curves do show a saturated slope for $m \geq 10$ in the scaling region, which corresponds to a correlation dimension of a chaotic attractor $n \approx 5-7$ (Figure 4b). Note that GP correlation dimension is an invariant of any chaotic attractor. Therefore, the consistent slopes of the correlation integrals in Figure 4 when m increases supports the existence of a chaotic attractor with dimension $n \approx 5-7$, sightly larger than what obtained from the LLE and SMC analyses but still within the same range of uncertainty.

In the search for the intrinsic dimension of TC chaotic attractor, we should recall a common underlying assumption that possible contributions from random noise must be sufficiently small. This is because noise could strongly interfere with the phase-space reconstruction and result in, e.g, an artificially positive LLE or incorrect correlation dimension estimation (Brock 1986; Sugihara et al. 1994; Casdagli 1992; Kantz and Schreiber 2003). The existence of noise in any model

[4]This correlation dimension algorithm is provided as a built-in function in Matlab's Predictive Toolbox.

output is natural even for deterministic systems because of the discretization or numeric errors in any model. How random noise impacts our phase-space reconstruction analyses of TC intensity is therefore elusive.

To address the robustness of our correlation dimension estimation in the presence of noise, one could employ different statistical testing methods or noise reduction algorithms that could distinguish the difference between chaotic and stochastic time series (Brock 1986; Baek and Brock 1992; Kantz and Schreiber 2003). Within the model simulation framework, we can however approach this problem differently by carrying out additional experiments in which random processes in the form of stochastic forcing are included in the CM1 model as described in Section 2. Any difference in the estimations of attractor invariants such as LLE, SMC, or correlation dimension between the stochastic and deterministic time series could therefore reveal the role of random noise in the TC intensity phase-space reconstruction.

In this regard, Figure 5 shows the derived correlation dimension n as a function of the embedding dimension m, which is obtained from the CM1 simulation with stochastic forcing implementation. Despite the existence of noise in the CM1 model, the correlation dimension shown in Figure 5 still displays a consistent behavior among all time series, similar to that obtained from the CM1 deterministic simulation in Figure 4. That is, n increases at first and but levels off for $m \geq 10$. This saturation of n with increasing embedding dimension m in the presence of noise is significant, because it indicates that the deterministic signals are more dominant, at least in the scaling region. As discussed in Kantz and Schreiber (2003), the random noise generally introduces extra dimensions to any deterministic chaos. As such, the result obtained in the CM1 stochastic simulation is required to establish the existence of TC intensity deterministic chaos, albeit the exact value of the TC intensity chaotic attractor is still not known.

We wish to note that the consistent behavior of the correlation dimension n between deterministic and stochastic simulations is only held for a certain range of noise amplitude. For a sufficiently large value of stochastic forcing, CM1 would crash due to violation of the model numerical stability, thus preventing us from examining to what extent random processes would dominate chaotic variability. Similar analyses of LLE or SMC for these stochastic simulations capture every similar results as shown in Figures 2-3, thus all together supporting the existence of low-dimensional chaos for TC intensity, even in the presence of random noise.

4. Discussion

From the deterministic dynamics perspective, the values of LLE (λ), the SMC de-correlation time (T^*), and the size of a bounded chaotic attractor (Γ) are all related, and they together dictate the range of intensity predictability. Indeed, assuming that an initial intensity error is ε_0, then the time required to reach the saturation level Γ, which is often considered as the range of predictability in practical applications, is given by $T_e = \frac{1}{\lambda} ln(\frac{\Gamma}{\varepsilon_0})$. If this interpretation of predictability in terms of the saturation time is rational, one would expect that T_e is of the same order of the magnitude as T^*. Assume for example $\Gamma \approx 8ms^{-1}$ from the real-time intensity verification (Tallapragada et al. 2014, 2015; Kieu and Moon 2016; Bhatia et al. 2017; Kieu et al. 2018, e.g.,), $\lambda = 1 \times 10^{-4} s^{-1}$, and $\varepsilon_0 = 0.5ms^{-1}$, one obtains $T_e \approx 8hrs$, which is of the same order of magnitude as T^* obtained from the Sugihara-May's decorrelation time scale (cf. Figure 3). Such consistency thus supports the nature of chaotic dynamics in determining TC intensity predictability as proposed in recent studies (Kieu and Moon 2016; Kieu et al. 2018; Kieu and Rotunno 2022).

Note however that unlike λ, T^*, or Γ, which can be considered as invariants of a chaotic attractor, the above estimation of T_e depends on the initial condition error ε_0. In principle, one could reduce ε_0 to as small a value as one wishes such that T_e can be arbitrarily long (Palmer et al. 2014).

However, the logarithm function in the estimation of T_e still imposes a strong constraint on the magnitude of T_e (i.e., a 10-time reduction in ε_0 can only lengthen T_e by ~ 2 times). Regardless of how long T_e is, it is eventually the de-correlation time T^* that puts a cut off on the intrinsic predictability of a chaotic system as discussed in Sugihara and May (1990), no matter how small ε_0 can be reduced. In this regard, the results obtained herein suggest a maximum range of 18-24 hours for TC intensity predictability, after reaching the mature stage.

Although the uncertainty in the estimation of LLE, SMC, or the range of intensity predictability as obtained from our analyses is significant and unavoidable, the fact that the existence of low-dimensional chaos for TC intensity can be confirmed from different angles as presented in this study is alone a profound finding. This is because TC nonlinear dynamics along with various physical parameterizations in any TC model make it impossible to directly derive any attractor from the governing equations. Therefore, the ability to capture such low-dimensional intensity chaos from a single time series of TC intensity is nontrivial. From the practical standpoint, the existence of low-dimensional chaos for TC intensity explains why forecasters usually characterize different TCs by using very few pieces of information such as V_{MAX}, P_{MIN}, storms size, warm core, or cloud top temperature. These pieces of information turn out to be sufficient to classify most TCs in practice without all other details, much like one can characterize the thermodynamics of a room with few bulk numbers such as temperature, density, or pressure. In this regard, the Takens embedding theorem is fundamental herein, as it guarantees that the phase-space reconstruction from TC intensity time series is feasible and meaningful if low-dimensional chaos exists.

5. Concluding remarks

Determining whether TC intensity has limited predictability, and if so, what is the maximum range of TC intensity predictability is of importance for operational forecast. In this study, the

phase-space reconstruction method was used to explore possible existence of low-dimensional chaos for TC intensity. Using the time series outputs from long TC simulations, we presented how the chaotic behaviors of TC dynamics could be examined from these time series.

With the outputs of wind and pressure variables extracted at the CM1 model maximum intensity equilibrium, it is found that TC intensity possesses indeed low-dimensional chaos from several perspectives. Specifically, our analyses of the largest Lyapunov exponent (LLE) and the Sugihara-May correlation (SMC) revealed a consistent positive LLE and a decaying SMC when the embedding dimension of the phase space $m \geq 10$ as expected for systems with low-dimensional chaos. For LLE, all estimations converge towards a rate in the range of $\sim 0.5 - 1 \times 10^{-4} s^{-1}$, which corresponds to an e-folding time of $\sim$ 1-3 hours for the wind variables and $\sim$ 3-6 hours for the pressure variable. Similarly, the SMC curve shows a consistent decaying of the predicted correlation after $\sim 1 - 5 \times 10^4 s$, regardless of the presence of random noise. These results together advocate that the variability in TC intensity time series is governed by chaotic dynamics, rather than pure stochastic fluctuation or projection of high-dimensional nonlinearity.

By cross-validating the convergence and the consistency of several attractor invariants including LLEs, SMCs, and the slopes of correlation integral, we estimated that the correlation dimension for TC intensity chaos attractor is in a range of [4-5]. This lower range indicates the existence of TC low-dimensional chaos at the maximum intensity equilibrium, thus offering some insights into why the use of minimum dynamical variables in the framework of TC scale phase space could reasonably represent TC dynamics as proposed in Kieu (2015); Kieu and Moon (2016); Kieu and Wang (2017). This result also helps explain the tendency of using just a few pieces of information such as V_{MAX}, P_{MIN}, storms size, warm core, or cloud top temperature to characterize different TCs in practice, instead of all possible detailed TC properties.

While the LLE and SMC measures depend on a certain choice of embedding dimension thresholds, model resolution, sampling frequency, or phase-space construction methods, it should be noted that our estimations of LLE and SMC are sufficiently robust for a range of sensitivity analyses. In particular, the convergence of LLE and SMC is consistent among the time series of all wind components and the minimum central pressure. Note, nevertheless, that the estimations of LLE and SMC from the time series of the minimum central pressure provide somewhat a smaller LLE value and a longer decorrelation time, as compared to those obtained from the time series of the wind components. This appears to be a notable property of TC dynamics, because it suggests then that the wind and the pressure variables tend to have a different range of predictability. The fact that a smaller LLE and a larger SMC time obtained from the pressure variable, in this regard, indicates that TC intensity would have a longer range of predictability if the minimum central pressure is used for intensity forecast.

Despite such difference between the mass and wind fields, the predictability range for TC intensity appears to be still within the range of 18-24 hours once TCs attain their quasi-stationary stage, depending on the criteria of intensity error saturation. These results provide concrete evidence about TC chaotic dynamics, and indicates that any future improvement of intensity accuracy should be based on different intensity metrics beyond the absolute intensity errors, regardless of how perfect our modelling system or observational networks would be in the future.

A number of caveats regarding the interpretation of TC intensity predictability obtained in this study should be cautioned here. First, the uncertainty in our estimations of all TC intensity chaotic invariants is significant, and to some extent, unavoidable as intensively discussed in Kantz and Schreiber (2003). This is because the choice of the embedding dimension and time delay for phase-space reconstruction, the existence of model/numeric noise as well as the finite sample size will all prevent one from obtaining the exact values of any deterministic invariants in any time series.

Our nonlinear time series analyses are therefore ad-hoc and contain some inherent subjectivity, especially in determining the convergence of deterministic invariants when varying the parameters in the phase-space reconstruction. As a result, the range of TC intensity predictability is rather broad as shown above.

Second, our estimation of the intensity predictability range is only applied to TC maximum intensity stage such that the stationary time series can be well maintained under fixed environmental conditions (i.e., the dynamics must be already on a chaotic attractor (Brock 1986; Kantz and Schreiber 2003; Alligood et al. 1996; Kieu and Moon 2016)). This restriction limits one from examining the variability of TC intensity during the early stage of development or as a function of environment. How TC intensity predictability depends on TC track or different intensity metrics beyond the few scalar variables used in this study is therefore still elusive.

Acknowledgments. This research was partially supported by the ONR/YIP Award N000141812588, ONR/DRI Award N000142012411. The corresponding author CK wishes to thank NOAA/GFDL and Princeton University for hosting his sabbatical visit in Fall 2021 during the preparation of this work.

Data Availability Statement

All time series generated from the CM1 simulations used in this study can be accessed from an online link here DOI:10.48550/arXiv.2110.05190.

References

Alligood, K. T., T. Sauer, and J. Yorke, 1996: *An Introduction to Dynamical Systems*. Springer-Verlag, New York, 603p.

Awrejcewicz, J., A. V. Krysko, N. P. Erofeev, V. Dobriyan, M. A. Barulina, and V. A. Krysko, 2018: Quantifying chaos by various computational methods. part 1: Simple systems. *Entropy*, **20 (3)**, doi:10.3390/e20030175.

Baek, E. G., and W. A. Brock, 1992: A nonparametric test for independence of a multivariate time series. *Statistica Sinica*, **01 (2)**, 137–156.

Balcerzak, M., D. Pikunov, and A. Dabrowski, 2018: The fastest, simplified method of lyapunov exponents spectrum estimation for continuous-time dynamical systems. *Nonlinear Dynamics*, **94**, 3053–3065.

Bhatia, K. T., D. S. Nolan, A. B. Schumacher, and M. DeMaria, 2017: Improving Tropical Cyclone Intensity Forecasts with PRIME. *Weather and Forecasting*, **32 (4)**, 1353–1377, doi:10.1175/WAF-D-17-0009.1.

Brock, W. A., 1986: Distinguishing random and deterministic systems: Abridged version. *Journal of Economic Theory*, **40 (1)**, 168–195, doi:https://doi.org/10.1016/0022-0531(86)90014-1.

Bryan, G. H., and J. M. Fritsch, 2002: A benchmark simulation for moist nonhydrostatic numerical models. *Monthly Weather Review*, **130 (12)**, 2917 – 2928, doi:10.1175/1520-0493(2002)130⟨2917:ABSFMN⟩2.0.CO;2.

Bryan, G. H., and R. Rotunno, 2009: The maximum intensity of tropical cyclones in axisymmetric numerical model simulations. *Mon. Wea. Rev.*, **137**, 1770–1789, doi:10.1175/2008MWR2709.1.

Bunker, R. C., A. E. Cohen, J. A. Hart, A. E. Gerard, K. E. Klockow-McClain, and D. P. Nowicki, 01 Apr. 2019: Examination of the predictability of nocturnal tornado events in the southeastern united states. *Weather and Forecasting*, **34 (2)**, 467 – 479, doi:10.1175/WAF-D-18-0162.1.

Casdagli, M., 1992: Chaos and deterministic versus stochastic non-linear modelling. *Journal of the Royal Statistical Society. Series B (Methodological)*, **54 (2)**, 303–328.

Christensen, H., I. Moroz, and T. Palmer, 2015: Stochastic and perturbed parameter representations of model uncertainty in convection parameterization. *J. Atmos. Sci.*, **72**, 2525–2544.

Davis, C. A., 2015: The formation of moist vortices and tropical cyclones in idealized simulations. *Journal of the Atmospheric Sciences*, **72 (9)**, 3499 – 3516, doi:10.1175/JAS-D-15-0027.1.

DelSole, T., 01 Oct. 2004: Predictability and information theory. part i: Measures of predictability. *Journal of the Atmospheric Sciences*, **61 (20)**, 2425 – 2440, doi:10.1175/1520-0469(2004)061⟨2425:PAITPI⟩2.0.CO;2.

DelSole, T., and M. K. Tippett, 2007: Predictability: Recent insights from information theory. *Reviews of Geophysics*, **45 (4)**, doi:https://doi.org/10.1029/2006RG000202, URL https://agupubs.onlinelibrary.wiley.com/doi/abs/10.1029/2006RG000202.

DelSole, T., L. Trenary, M. K. Tippett, and K. Pegion, 15 May. 2017: Predictability of week-3–4 average temperature and precipitation over the contiguous united states. *Journal of Climate*, **30 (10)**, 3499 – 3512, doi:10.1175/JCLI-D-16-0567.1, URL https://journals.ametsoc.org/view/journals/clim/30/10/jcli-d-16-0567.1.xml.

Dorrestijn, J., D. Crommelin, H. J. A.P. Siebesma, and C. Jakob, 2015: Stochastic parameterization of convective area fractions with a multicloud model inferred from observational data. *J. Atmos. Sci.*, **72**, 854–869.

Durran, D. R., P. A. Reinecke, and J. D. Doyle, 2013: Large-scale errors and mesoscale predictability in pacific northwest snowstorms. *Journal of the Atmospheric Sciences*, **70 (5)**, 1470 – 1487, doi:10.1175/JAS-D-12-0202.1.

Emanuel, K. A., 1986: An air-sea interaction theory for tropical cyclones. part i: Steady-state maintenance. *J. Atmos. Sci.*, **43**, 585–605.

Fraser, A. M., and H. L. Swinney, 1986: Independent coordinates for strange attractors from mutual information. *Phys. Rev. A*, **33**, 1134–1140, doi:10.1103/PhysRevA.33.1134, URL https://link.aps.org/doi/10.1103/PhysRevA.33.1134.

Goswami, B. N., K. Rajendran, and D. Sengupta, 01 May. 1997: Source of seasonality and scale dependence of predictability in a coupled ocean–atmosphere model. *Monthly Weather Review*, **125 (5)**, 846 – 858, doi:10.1175/1520-0493(1997)125⟨0846:SOSASD⟩2.0.CO;2.

Grassberger, P., T. Schreiber, and C. Schaffrath, 1991: Nonlinear time sequence analysis. *International Journal of Bifurcation and Chaos*, **01 (03)**, 521–547, doi:10.1142/S0218127491000403.

Hakim, G. J., 2011: The mean state of axisymmetric hurricanes in statistical equilibrium. *Journal of the Atmospheric Sciences*, **68 (6)**, 1364–1376, doi:10.1175/2010jas3644.1, URL https://doi.org/10.1175/2010JAS3644.1.

Hakim, G. J., 2013: The variability and predictability of axisymmetric hurricanes in statistical equilibrium. *Journal of the Atmospheric Sciences*, **70 (4)**, 993–1005, doi:10.1175/jas-d-12-0188.1, URL https://doi.org/10.1175/JAS-D-12-0188.1.

Hart, J. A., and A. E. Cohen, 2016a: The challenge of forecasting significant tornadoes from june to october using convective parameters. *Wea. Forecasting*, **31**, 2075–2084.

Kantz, H., 1994: A robust method to estimate the maximal lyapunov exponent of a time series. *Physics Letters A*, **185 (1)**, 77–87, doi:https://doi.org/10.1016/0375-9601(94)90991-1.

Kantz, H., and T. Schreiber, 2003: *Nonlinear Time Series Analysis*. 2nd ed., Cambridge University Press, doi:10.1017/CBO9780511755798.

Kieu, C., 2015: Hurricane maximum potential intensity equilibrium. *Q.J.R. Meteorol. Soc.*, **141 (692)**, 2471–2480, doi:10.1002/qj.2556.

Kieu, C., C. Evans, Y. Jin, J. D. Doyle, H. Jin, and J. Moskaitis, 2021: Track dependence of tropical cyclone intensity forecast errors in the coamps-tc model. *Weather and Forecasting*, **36 (2)**, 469 – 485, doi:10.1175/WAF-D-20-0085.1.

Kieu, C., and R. Rotunno, 2022: Characteristics of tropical-cyclone turbulence and intensity predictability. *Geophysical Research Letters*, **49 (8)**, e2021GL096 544, doi:https://doi.org/10.1029/2021GL096544, e2021GL096544 2021GL096544.

Kieu, C. Q., K. Keshavamurthy, V. Tallapragada, S. Gopalakrishnan, and S. Trahan, 2018: On the growth of intensity forecast errors in the operational hurricane weather research and forecasting (hwrf) model. *Quarterly Journal of the Royal Meteorological Society*, **144 (715)**, 1803–1819, doi:10.1002/qj.3344, URL https://rmets.onlinelibrary.wiley.com/doi/abs/10.1002/qj.3344, https://rmets.onlinelibrary.wiley.com/doi/pdf/10.1002/qj.3344.

Kieu, C. Q., and Z. Moon, 2016: Hurricane Intensity Predictability. *Bull. Amer. Meteor. Soc.*, doi:10.1175/BAMS-D-15-00168.1.

Kieu, C. Q., and Q. Wang, 2017: Stability of tropical cyclone equilibrium. *J. Atmos. Sci.*, **74**, 3591–3608.

Klotzbach, P. J., M. M. Bell, S. G. Bowen, E. J. Gibney, K. R. Knapp, and C. J. Schreck, 2020: Surface pressure a more skillful predictor of normalized hurricane damage than maximum sustained wind. *Bulletin of the American Meteorological Society*, **101 (6)**, E830 – E846, doi:10.1175/BAMS-D-19-0062.1.

Leith, C. E., 1971: Atmospheric predictability and two-dimensional turbulence. *J. Atmos. Sci.*, **28**, 145–161.

Lorenz, E. N., 15 Dec. 1992: The slow manifold—what is it? *Journal of Atmospheric Sciences*, **49 (24)**, 2449 – 2451, doi:10.1175/1520-0469(1992)049⟨2449:TSMII⟩2.0.CO;2.

Lorenz, E. N., 1969: The predictability of a flow which possesses many scales of motion. *Tellus A*, **21A**, 289–307.

Lorenz, E. N., 1990: *Predictability - A problem partly solved. Predictability of Weather and Climate*. Tim palmer and renate hagedorn ed., Cambridge University Press.

Lorenz, E. N., 1996: PREDICTABILITY-A PROBLEM PARTLY SOLVED. *Preprint*, URL http://eaps4.mit.edu/research/Lorenz/misc_lorenz_1996_predictability_problem_partly_solved.pdf.

Métais, O., and M. Lesieur, 1986: Statistical Predictability of Decaying Turbulence. *J. Atmos. Sci.*, **43 (9)**, 857–870, doi:10.1175/1520-0469(1986)043⟨0857:SPODT⟩2.0.CO;2, URL http://journals.ametsoc.org/doi/abs/10.1175/1520-0469(1986)043%3C0857%3ASPODT%3E2.0.CO%3B2.

Montgomery, M. T., v. s. nguyen, j. persing, and r. k. smith, 2009: do tropical cyclones intensify by wishe? *q. j. r. meteorol. soc*, **135**, 1697–1714.

Nguyen, P., C. Q. Kieu, and W.-T. L. Fan, 2020: Stochastic Variability of Tropical Cyclone Intensity at the Maximum Potential Intensity Equilibrium. *Journal of the Atmospheric Sciences*, **77 (9)**, 3105–3118, doi:10.1175/JAS-D-20-0070.1.

Nicolis, C., and G. Nicolis, 1984: Is there a climatic attractor? *Nature*, **311**, 529–532, doi:https://doi.org/10.1038/311529a0.

Palmer, T. N., 2001: A nonlinear dynamical perspective on model error: A proposal for non-local stochastic–dynamic parametrization in weather and climate prediction models. *Quart. J. Roy. Meteor. Soc*, **127**, 279–304.

Palmer, T. N., A. Doring, and G. Seregin, 2014: The real butterfly effect. *Nonlinearity*, **27**, 123–141.

Rhodes, C., and M. Morari, 1997: False-nearest-neighbors algorithm and noise-corrupted time series. *Phys. Rev. E*, **55**, 6162–6170, doi:10.1103/PhysRevE.55.6162.

Rosenstein, M. T., J. J. Collins, and C. J. De Luca, 1993: A practical method for calculating largest lyapunov exponents from small data sets. *Physica D: Nonlinear Phenomena*, **65 (1)**, 117–134, doi:https://doi.org/10.1016/0167-2789(93)90009-P.

Rotunno, R., and K. A. Emanuel, 1987: An air–sea interaction theory for tropical cyclones. part ii: Evolutionary study using a nonhydrostatic axisymmetric numerical model. *J. Atmos. Sci.*, **44**, 542–561.

Schneider, T., and S. M. Griffies, 1999: A conceptual framework for predictability studies. *Journal of Climate*, **12**, 3133–3155.

Shukla, J., 1981: Dynamical predictability of monthly means. *Journal of Atmospheric Sciences*, **38 (12)**, 2547 – 2572, doi:10.1175/1520-0469(1981)038⟨2547:DPOMM⟩2.0.CO;2.

Stensrud, D. J., and Coauthors, 01 Oct. 2009: Convective-scale warn-on-forecast system: A vision for 2020. *Bulletin of the American Meteorological Society*, **90 (10)**, 1487 – 1500, doi:10.1175/2009BAMS2795.1.

Sugihara, G., B. T. Grenfell, R. M. May, and H. Tong, 1994: Nonlinear forecasting for the classification of natural time series. *Philosophical Transactions of the Royal Society of London. Series A: Physical and Engineering Sciences*, **348 (1688)**, 477–495, doi:10.1098/rsta.1994.0106.

Sugihara, G., and R. May, 1990: Nonlinear forecasting as a way of distinguishing chaos from measurement error in time series. *Journal of Economic Theory*, **344**, 734–741, doi:https://doi.org/10.1038/344734a0.

Takens, F., 1981: *Detecting strange attractors in turbulence. Rand D., Young LS. (eds) Dynamical Systems and Turbulence, Warwick 1980*. Springer-Verlag, Berlin, Heidelberg, lecture Notes in Mathematics.

Tallapragada, V., C. Q. Kieu, Y. Kwon, S. Trahan, Q. Liu, Z. Zhang, and I.-H. Kwon, 2014: Evaluation of Storm Structure from the Operational HWRF during 2012 Implementation. *Mon. Wea. Rev.*, **142**, 4308–4325, doi:10.1175/MWR-D-13-00010.1.

Tallapragada, V., and Coauthors, 2015: Forecasting Tropical Cyclones in the Western North Pacific Basin using the NCEP Operational HWRF Model. Model Upgrades and Evaluation of Real-Time Performance in 2013. *Wea. Forecasting*, doi:10.1175/WAF-D-14-00139.1.

Theiler, J., 1987: Efficient algorithm for estimating the correlation dimension from a set of discrete points. *Physical Review A*, **36**, 44–56.

Wallot, S., and D. Monster, 2018: Calculation of average mutual information (ami) and false-nearest neighbors (fnn) for the estimation of embedding parameters of multidimensional time series in matlab. *Frontiers in Psychology*, **9**, 1679, doi:10.3389/fpsyg.2018.01679.

Wang, Y., 2001: An explicit simulation of tropical cyclones with a triply nested movable mesh primitive equation model: Tcm3. part i: Model description and control experiment. *Monthly*

Weather Review, **129 (6)**, 1370 – 1394, doi:10.1175/1520-0493(2001)129⟨1370:AESOTC⟩2.0.CO;2.

Wolf, A., J. B. Swift, H. L. Swinney, and J. A. Vastano, 1985: Determining lyapunov exponents from a time series. *Physica D: Nonlinear Phenomena*, **16 (3)**, 285–317, doi:https://doi.org/10.1016/0167-2789(85)90011-9, URL https://www.sciencedirect.com/science/article/pii/0167278985900119.

Zhang, F., C. Snyder, and R. Rotunno, 2003: Effects of moist convection on mesoscale predictability. *Journal of the Atmospheric Sciences*, **60 (9)**, 1173 – 1185, doi:10.1175/1520-0469(2003)060⟨1173:EOMCOM⟩2.0.CO;2.

Zhang, Z., V. Tallapragada, C. Kieu, S. Trahan, and W. Wang, 2015: Hwrf based ensemble prediction system using perturbations from gefs and stochastic convective trigger function. *Tropical Cyclone Research and Review*, **3**, 145–161.

LIST OF FIGURES

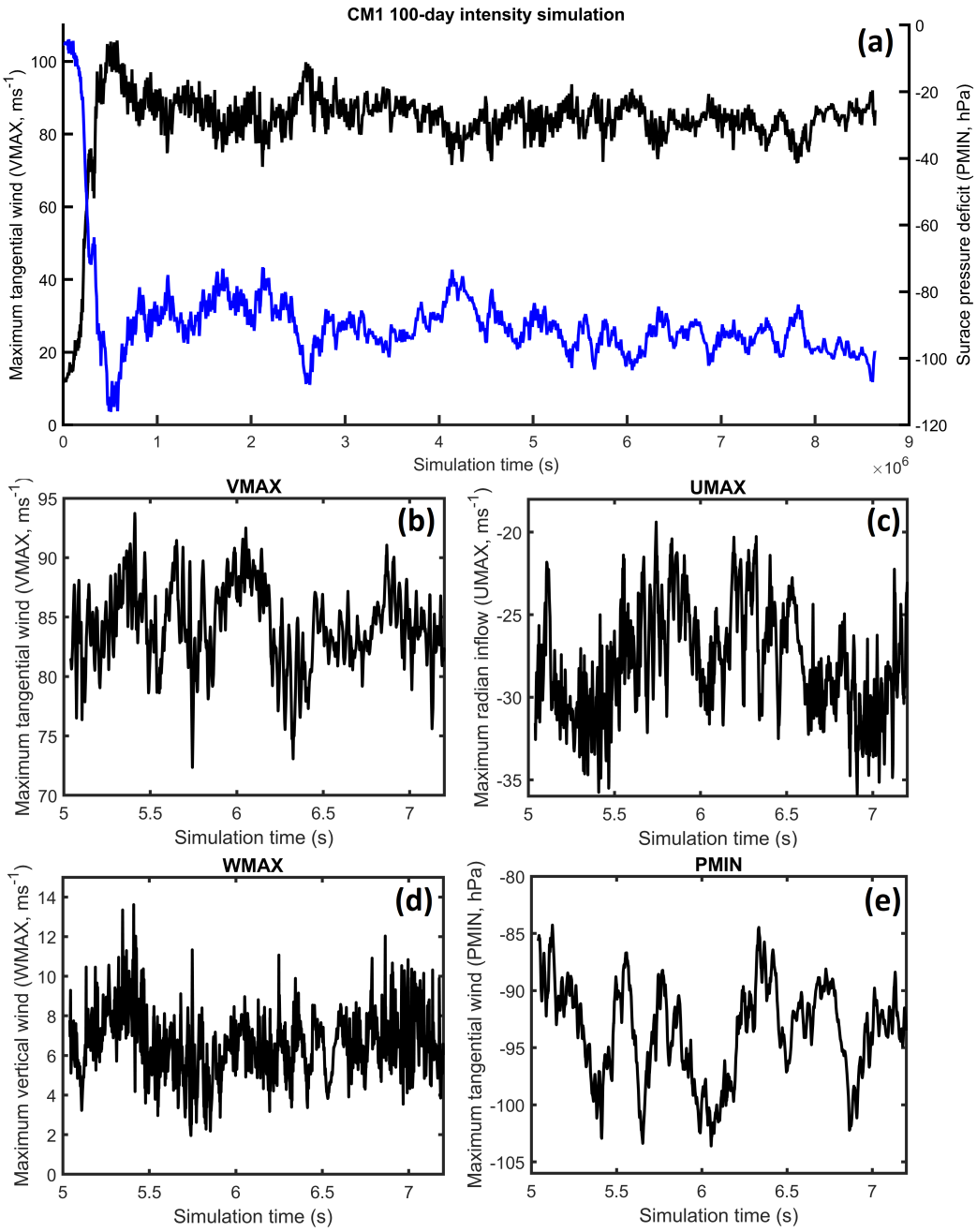

FIG. 1. (a) Time series of the maximum surface wind V_{MAX} (black, unit ms^{-1}) and the minimum surface pressure deficit P_{MIN} (blue, unit hPa) from an 100-day simulations using the CM1 model; (b) A close-up window of the V_{MAX} time series during the maximum intensity equilibrium from day 57-81 of the CM1 simulation; (c)-(d) similar to (b) but for the maximum radial inflow at the surface U_{MAX}, the maximum vertical motion in the eyewall region W_{MAX} and P_{MIN}, respectively.

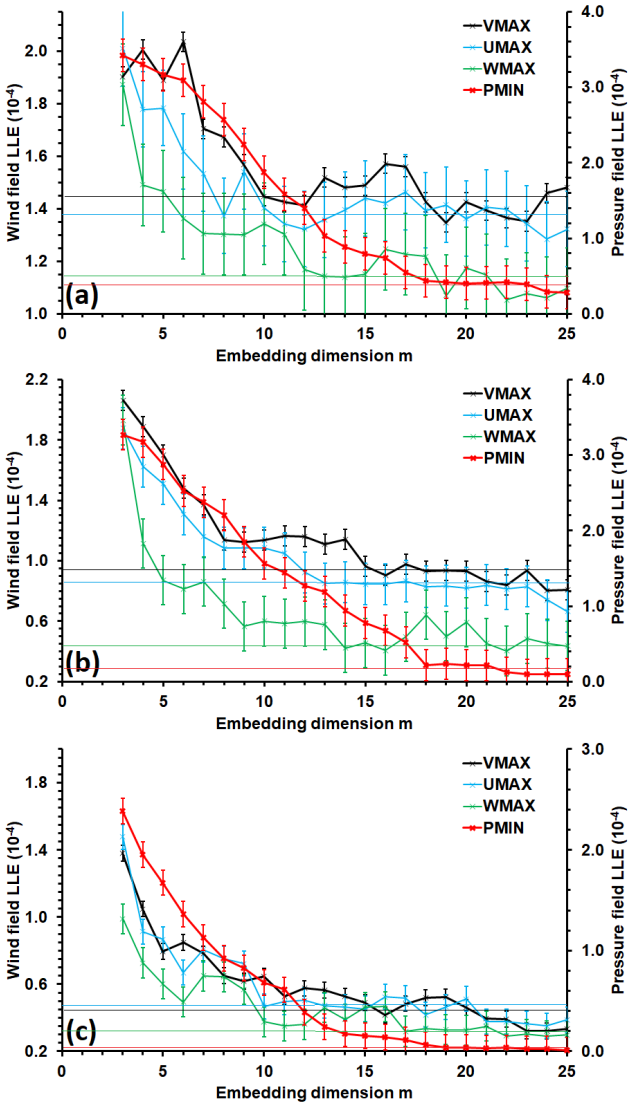

FIG. 2. Dependence of the largest Lyapunov exponent (LLE, unit $10^{-4}s^{-1}$) on the embedding dimension m for V_{MAX} (black), U_{MAX} (cyan), W_{MAX} (green) and P_{MIN} (red, right axis) for (a) delay time $\tau = 10$ *mins*, (b) $\tau = 30$ *mins*, and (c) $\tau = 45$ *mins*. Error bars denote the 95% confidence intervals obtained during the maximum intensity equilibrium. Thin solid lines indicate the asymptotic values that LLEs approach when m increases.

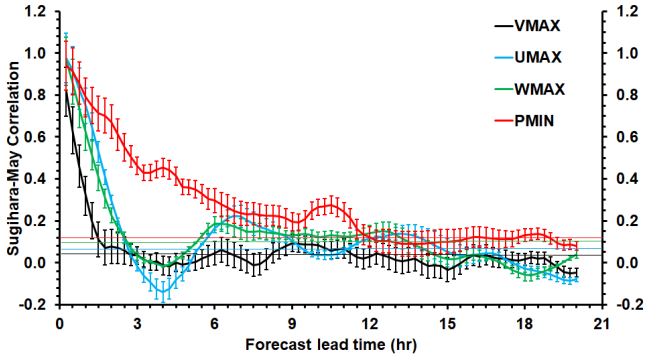

FIG. 3. Dependence of the Sugihara-May correlation (SMC) on the forecast lead time T for V_{MAX} (black), U_{MAX} (cyan), W_{MAX} (green) and P_{MIN} (red). Error bars denote the 95% confidence intervals obtained during the maximum intensity equilibrium.

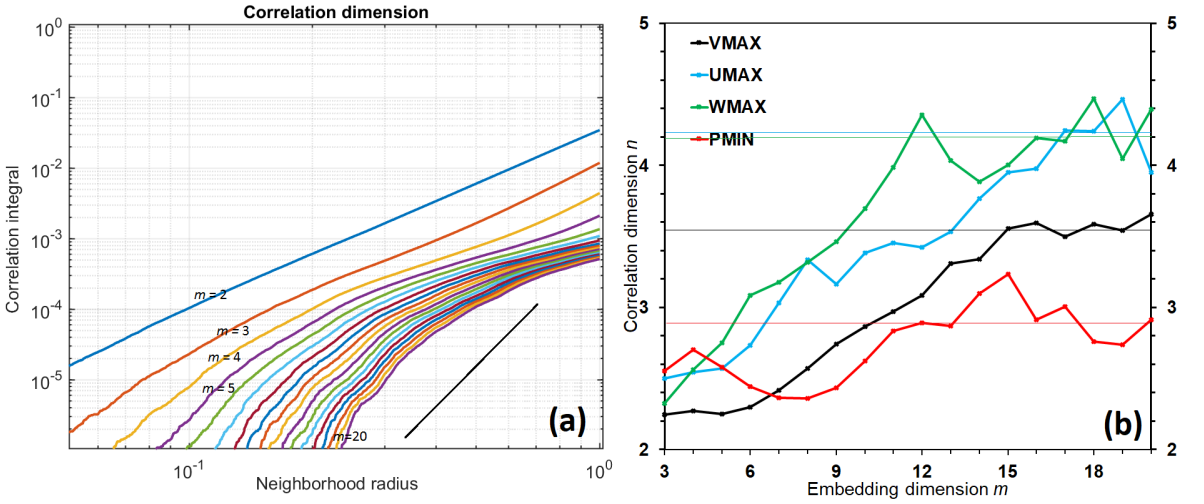

FIG. 4. (a) Dependence of the V_{MAX} correlation integral on the neighborhood radius for a range of embedding dimension m from 2-20; and (b) the dependence of the slope of the correlation integral-radius curve in (a) on the embedding dimension m as obtained from V_{MAX} (black), U_{MAX} (cyan), W_{MAX} (green) and P_{MIN} (red) time series. The black line denotes the saturated slope of the correlation integral curves at the scaling region.

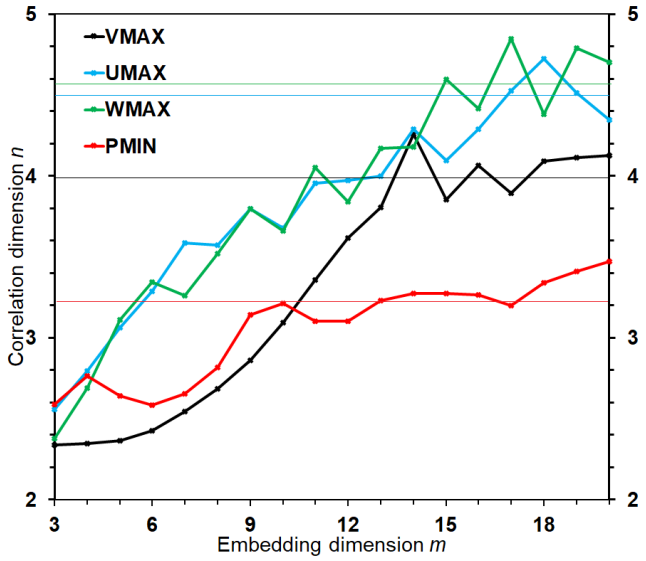

FIG. 5. Similar to Figure 4b but for the CM1 simulation in which additive random noises are added to model wind fields at every time step of the model integration over the entire model domain.